

Article

The Adsorption Performance of Porous Activated Carbons Prepared from Iron (II) Precursors Precipitated on the Porous Carbon Matrix Thermolysis

Alexander Kalenskii, Aleksey Ivanov, Dmitriy Sevostyanov, Alexander Zvekov * and Alexander Krechetov

Department of Solid State Chemistry and Material Science, Kemerovo State University, Krasnaya, 6, 650000 Kemerovo, Russia; kalenskyav@gmail.com (A.K.); alecs-2004@yandex.ru (A.I.); vp-1990@bk.ru (D.S.); alex.krech@yandex.ru (A.K.)

* Correspondence: zvekova@gmail.com; Tel.: +8-909-515-32-64

Abstract: The creation of new compounds featuring high adsorption and catalytic performance with magnetic properties of the material is one of the important fields of magnetochemistry. The typical synthetic schemes of magnetic carbonaceous adsorbents are rather complicated due to the use of inert atmosphere and difficult wet methods of magnetite precipitation. The arising experimental issues prevent industrial production of magnetically activated carbons. In order to overcome these obstacles, we suggested a novel approach to porous carbons: magnetite composite synthesis based on iron (II) salt precipitation on porous carbon and subsequent thermolysis. We facilitated the process at the stage of the material washing. The synthetic route used is simple and can be applied industrially. The present paper is focused on the adsorption performance of a product prepared from commercial activated carbons BAU-A and AG-3. The porous structure was studied with low-temperature nitrogen adsorption that revealed surface area decreased by 26% in the case of BAU-A and 40% in the case of AG-3 with an increase in mesopore volume. Phenol and nitrobenzene adsorption from water solution was tested with magnetic carbon prepared from BAU-A. The adsorption isotherms obtained are described well using the Langmuir model. The limiting adsorption value in the case of magnetic porous carbon is lower than in the case of pristine carbon. The relative decrease in limiting adsorption value is close to the relative decrease in the specific surface area. The adsorption constant remains the same, showing that adsorption centers of phenol and nitrobenzene are the same for porous magnetic carbon and its activated carbon precursor. Thus, we showed in the present study that the magnetically activated carbons we developed almost retain the adsorption performance of their activated carbon precursors.

Keywords: magnetic adsorbent; magnetite; thermolysis; adsorption performance



Citation: Kalenskii, A.; Ivanov, A.; Sevostyanov, D.; Zvekov, A.; Krechetov, A. The Adsorption Performance of Porous Activated Carbons Prepared from Iron (II) Precursors Precipitated on the Porous Carbon Matrix Thermolysis. *Magnetochemistry* **2023**, *9*, 151. <https://doi.org/10.3390/magnetochemistry9060151>

Academic Editor: Victor M. García-Suárez

Received: 5 May 2023

Revised: 2 June 2023

Accepted: 5 June 2023

Published: 8 June 2023



Copyright: © 2023 by the authors. Licensee MDPI, Basel, Switzerland. This article is an open access article distributed under the terms and conditions of the Creative Commons Attribution (CC BY) license (<https://creativecommons.org/licenses/by/4.0/>).

1. Introduction

The development of composite materials combining different properties in one body is one of the most significant trends of contemporary material science. Magnetochemistry aims at the creation of new compounds featuring high adsorption [1] and catalytic performance [1,2] with magnetic properties of the material.

Porous carbon-based materials containing magnetite are used extensively due to their high adsorption performance [3] and significant electric double layer capacity [4]. The preparation of magnetic adsorbents is relevant to various natural and technological systems, including the purification of oil processing products [5–7] and heavy metal ions [5,7,8]. These adsorbents are made from polymers [6], wood fibers [4], sulfated fatty [7] and humic acids [8], etc. Inorganic magnetic particles are able to efficiently adsorb metal ions from aqueous media even without current carriers [9].

The microconcentration of impurities to prepare them for qualitative and quantitative analysis is another relevant application area of magnetic adsorbents. A magnetic

adsorbent for cadmium and lead microextraction based on carbon nanotubes modified with benzothiazoline-2-thione was created in [10]. A special adsorbent for lead extraction from aqueous media based on carbon nanotubes and cross-linked dithizone containing polymer as a ligand was developed in [11]. A synthetic method of producing (3-Mercaptopropyl)trimethoxysilane—multiwalled carbon nanotubes—magnetite applied for mercury and lead extraction was suggested in [12]. An adsorbent containing zinc ferrite for organic pollutant (such as bisphenol A, antibiotics, herbicides, and some others) microconcentration was prepared in [13] via metal–organic framework carbonization.

The most common approach to magnetic adsorbent synthesis is based on magnetic particle precipitation to the highly porous carbonaceous matrix [10,14]. Magnetite precipitation onto carbon nanotubes from an ammonium iron (III) sulfate solution and subsequent reduction with hydrazine hydrate was performed in [9]. The precipitation of magnetite from an iron (III) pentanedionate-2,4 solution onto multi-walled carbon nanotubes in the presence of triethylene glycole was performed in an argon atmosphere [12]. The precipitation of magnetite onto commercial nanotubes from a solution containing ammonium iron (II) sulfate and iron (III) chloride with ammonia in a nitrogen atmosphere was performed in [14]. A carbonaceous adsorbent based on pomelo peels with magnetite deposition from an iron (II) and (III) salt solution with ethylenediamine bubbled with nitrogen was prepared in [15]. Its performance in paraben and fluoroquinolone concentration for high-performance liquid chromatography analysis was studied.

Ferrites are considered an alternative to magnetite. The method of zinc ferrite nanoparticle encapsulation in a carbon shell as a result of metal–organic framework carbonization was suggested in [13]. These encapsulated particles showed themselves as an efficient adsorbent for antibacterial substances [13]. An adsorbent for tetracycline extraction from aqueous medium based on multi-walled carbon nanotubes modified with manganese ferrite was prepared in [16]. It is worth mentioning that ferrites with extensive surface area are able to adsorb a number of inorganic pollutants from aqueous media [17].

Magnetite–clay minerals composites are another important type of magnetic adsorbent which are useful for both inorganic [18] and organic [19] pollutants. The procedure of magnetite deposition is close to the one used in the case of activated carbons, so the inertial atmosphere remains essential [19]. In the case of [18], the activation was performed using iron oxides, leading to rather low specific surface area (172 m²/g).

A mechanochemical synthetic method of carbonaceous adsorption from the past composed of magnetic particles and carbonized lignite was proposed in [20]. The authors of the paper [4] suggested magnetite deposition onto starch followed by its carbonization, aiming at electrode material preparation. An effective method of organic substance adsorbent preparation from fossil carbon based on its semicoking followed by activation with potassium hydroxide and iron (III) chloride was suggested in [3]. The last stage was performed at 800 °C in a vacuumed furnace. A number of magnetic adsorbent preparation schemes from biomass and other available sources were discussed in [21].

Thus, most magnetic carbonaceous adsorbent synthesis methods developed nowadays are focused on magnetite deposition onto a carbonaceous porous matrix. The existence of iron (II) compounds in the reaction medium that are readily oxidized in water solutions makes it essential to meet strict requirements for pH and temperature maintenance, as well as the use of an inert atmosphere. Negligible changes in reaction conditions make it possible to synthesize antiferromagnetic vustite, paramagnetic hematite, or slightly magnetic maghemite instead of magnetite, whose magnetism is the most pronounced among iron oxides. The process complexity explains the applicability of most methods at the laboratory scale, whereas their scaling is extremely difficult. For that reason, the development of new approaches for magnetic carbonaceous adsorbent synthesis free of the drawbacks mentioned above is a problem of both scientific and practical relevance.

Magnetite is a decomposition product of some labile iron substances. The iron (II) oxalate thermal decomposition in the production atmosphere was studied in [22] using thermal analysis techniques, differential scanning calorimetry, Mössbauer spectroscopy,

and X-ray diffraction. It was shown that the decomposition of iron (II) oxalate begins at 360 °C with the following main products: magnetite (80%) and cementite (20%) at 400 °C, cementite turns to α -iron at 500 °C, and magnetite turns to vustite at temperatures higher than 550 °C [22]. It was underlined that most magnetite at 400 °C exists in the superparamagnetic state [22]. To summarize, the authors of [22] demonstrated the applicability of labile iron substance decomposition as a prospective method of magnetite synthesis. We used this option in [19] for magnetite deposition onto activated carbon. It was shown with X-ray diffraction that magnetite is the substance deposited [23]. The product obtained effectively adsorbs benzene vapor and methylene blue from water solution [23]. The aim of the present work is to determine the porous structure parameters and test the adsorption performance of a carbonaceous magnetic adsorbent prepared via iron (II) oxalate thermolysis.

Phenol and nitrobenzene, which are typical environmental pollutants in regions of extensive chemical industry, were used as adsorbates. The maximum permissible concentration of phenol in potable water is 0.001 mg/L, according to the recommendations applicable in the USA and Russia. The maximum permissible concentration of nitrobenzene is higher, being 0.2 mg/L.

2. Materials and Methods

2.1. Synthesis of the Magnetic Adsorbent

Iron (II) sulfate heptahydrate and potassium oxalate monohydrate, both chemically pure, were used for magnetite synthesis. The activated carbons BAU-A and AG-3 were applied as model porous carbonaceous matrices.

The activated carbons were crushed in a mortar and sifted, taking the fraction 0.1–0.5 mm for further utilization. The activated carbon in the air-dry state with mass 2 g was placed in a beaker. A solution of FeSO₄ (1 M) was added and a solution of K₂C₂O₄ (1 M) was added next, stirring the mixture [23]. The volumes of the iron (II) sulfate and potassium oxalate are listed in Table 1. Yellow to orange iron (II) oxalate precipitated. The mixture was washed via decantation and filtered through white ribbon filter paper. The intermediate compound was dried at 120–130 °C. The dried compound was calcined in a crucible sealed with aluminum foil for 2 hours at 400 °C in a muffle oven. The black product of calcinations hold with a magnet was washed in a beaker with distilled water and ethanol, aiming at the visual purity of poured-out water. The product was filtrated using a Büchner funnel and dried in a drying oven at 110 °C. As a result, 2.5 g of magnetic adsorbent was produced from 2 g of activated carbon. The yield estimated in the assumption of quantitative iron transition to magnetite is 70%. The photo of the adsorbent collected with the magnetite while washing is shown in Figure 1. The synthesized adsorbent appeared as a black powder attracted to a stationary magnet. The granulometric distribution of the activated carbon precursor was not affected by the magnetite deposition.

Table 1. Porous structure parameters of the initial activated carbons and prepared magnetic adsorbents.

No.	Sample	V _{FeSO₄} , mL	V _{K₂C₂O₄} , mL	A _{SBV} , mg/g	A _{MB} , mg/g	S _{BET} , m ² /g	V _Σ , cm ³ /g	V _{micro} , cm ³ /g	V _{meso} , cm ³ /g	D _{pores} , Å
1	BAU-A	-	-	250	100	576	0.280	0.185	0.074	19
2	AG-3	-	-	185	152	621	0.317	0.129	0.067	20
3	BAU-A-M0.5	10	15	-	-	579	0.297	0.183	0.090	20
4	BAU-A-M	20	30	230	68	426	0.282	0.132	0.134	26
5	AG-3-M	20	30	136	143	370	0.279	0.068	0.141	30



Figure 1. Magnetic adsorbent during the washing stage, showing its attraction to a stationary magnet.

2.2. Porous Structure Research

The porous structure parameters were researched using the following methods: saturated benzene vapor (SBV) adsorption, methylene blue (MB) adsorption from aqueous medium, and low-temperature nitrogen adsorption. Benzene adsorption was measured via mass increase of the dried adsorbent sample held in a closed desiccator with an open benzene-containing vessel for at least 24 h. Methylene blue was adsorbed with 0.1 g of the adsorbent from 25 mL of aqueous solution at 1.5 g/L concentration, stirred for 20 min. The methylene blue concentration was determined spectrophotometrically using a Shimadzu UV-2450 spectrophotometer.

The porous structure was studied with the low-temperature nitrogen adsorption method using vacuumed static facility ASAP-2020 Micromeritics. The specific surface area (S_{BET} , m^2/g) was determined via nitrogen N_2 adsorption–desorption isotherm analysis at 77 K. The samples were dried in a drying oven at 105 ± 5 °C until constant mass was reached; they were then vacuumed in a special facility port at 110 °C for 12 h up to residual pressure 5×10^{-3} mmHg. The adsorption–desorption of nitrogen isotherms was measured within the equilibrium relative pressure range P/P_0 from 0.001 to 0.995 at the absolute temperature 77 K. The specific surface area was calculated according to the Brunauer–Emmett–Teller model (BET). The micropore volume was determined using the t-plot comparative method. The mesopore volume and size distribution were estimated using the Barrett–Joyner–Halenda approach (BJH). The average pore diameter was estimated as $D_{pores} = 4V_{\Sigma}/S$ using BET data. The typical uncertainty of the porous structure parameters was 5–7%.

2.3. Phenol and Nitrobenzene Adsorption from Aqueous Medium

Solutions of phenol and nitrobenzene were prepared using distilled water as a solvent. Activated carbon BAU-A or magnetic adsorbent on its base was dried in the drying oven at 80 °C up to constant mass. The dried adsorbent (50 mg) was placed in a flask and the adsorbate solution was added. The sealed flasks were stirred for 2 h. The adsorbate concentration in the solution equilibrated this way with the adsorbent was determined spectrophotometrically using the standard curves method. Stirring for less than 2 h does not lead to adsorption equilibrium reached in the preliminary experiments. The determination was done at the wavelength 261 nm for nitrobenzene ($\epsilon = 7500 \pm 200$ L/(mole·cm)) and 269 nm for phenol ($\epsilon = 1530 \pm 40$ L/(mole·cm)). The confidence interval was estimated at the confidential probability 95% here and further. The typical UV light-absorption spectrum of phenol solution reached the adsorption equilibrium via stirring with activated carbon BAU-A is shown on Figure 2. The constant increment in the visible range appears after stirring due to fine suspended particles of activated carbon. In the case of activated carbons, as well as for many carbonaceous materials, optical density is almost independent of the wavelength, so we additionally measured optical density at 800 nm and subtracted it from the solution's optical density at the maximum of the adsorbate band.

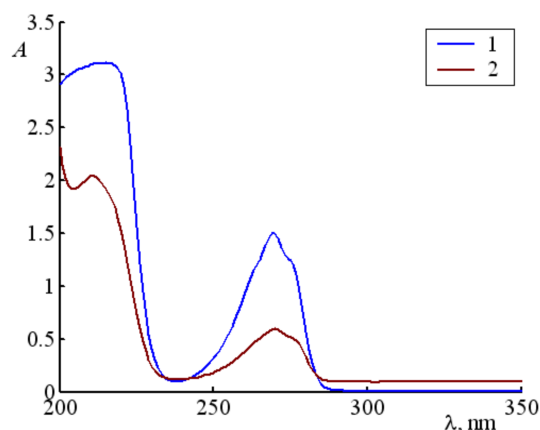


Figure 2. The measured UV light absorption spectra of phenol 1 mM (1) and solution equilibrated with activated carbon BAU-A with stirring (2).

In the case of phenol adsorption onto the magnetic adsorbent, the following typical UV light absorption spectra were measured (Figure 3). Similar spectra were observed in case of nitrobenzene. Comparing Figures 2 and 3, one notices that in the case of magnetic adsorbent, adsorbate bands are overlapped with continuous light-absorption linked with the magnetic activated carbon. The light absorption spectrum of a colloid obtained with magnetic adsorbent (50 mg) stirring in water (50 mg) and sedimentation of the rough fraction for 1 h is presented on Figure 4. The monotonic increase in the optical density with the decrease in wavelengths is evident in the UV region. A shoulder is observed in the range 260–270 nm, matching the phenol and nitrobenzene absorption band maximums. The diffuse reflectance spectra of the set of iron oxides were measured in [24], and it was revealed that absorptivity increases in the range of 750–900 nm for every oxide apart from magnetite. Fine black powder could be concentrated on the wall of the glass vessel with constant magnet action for a day. These two reasons evidence that the increment in the optical density observed is linked to fine magnetite particles.

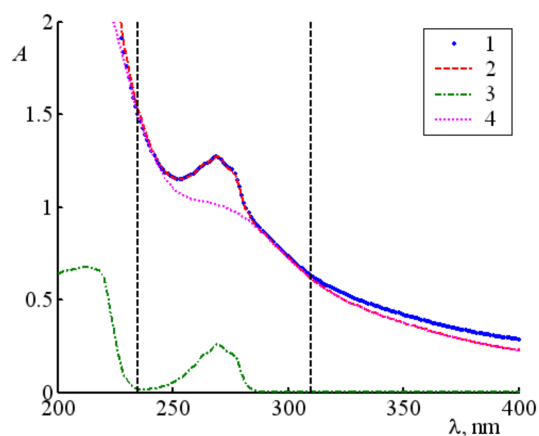


Figure 3. The UV light absorption spectrum of phenol solution equilibrated with magnetic adsorbent with stirring (1), its approximation (2), the parts of phenol (3) and magnetite fine particles (4) in the light absorption.

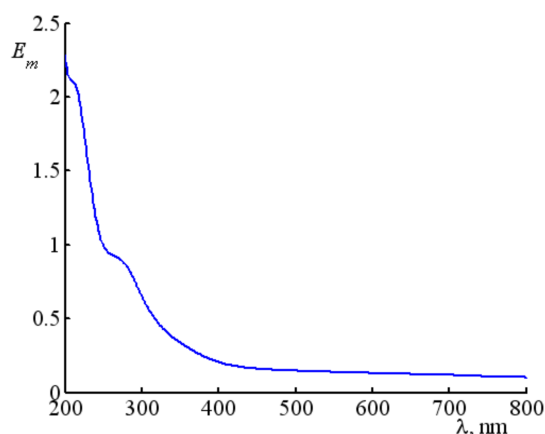


Figure 4. The UV light absorption spectrum of the colloid solution prepared with magnetic adsorbent stirring in distilled water and sedimentation of the big particles for 1 h.

The match of the adsorbate's UV light absorption band position and the shoulder on the fine magnetite particle spectrum makes it difficult to use the base line or Brice–Schwinn methods [25]. For that reason, the following approach was applied. It was assumed that optical density spectral dependence in the solution after reaching the adsorption equilibrium with magnetic adsorbent could be described as a superposition of adsorbates and fine magnetite in the range 230–340 nm whose contributions were taken as variables:

$$\frac{A(\lambda)}{l} = \varepsilon_a(\lambda) C_a + E_m(\lambda) C_m$$

where l is the cuvette thickness, C_a and $\varepsilon(\lambda)$ are molar concentration and molar absorption coefficient of the adsorbate, and c_m and $E_m(\lambda)$ are relative concentration and optical density of the system obtained as a result of magnetic adsorbent stirring in distilled water.

The best approximation was achieved using the least squares method in two ways. The first one was based on the minimizations of least-squares deviations of the experimental and calculated optical density, with the Nelder–Mead method determining the values C_a and c_m . In terms of the second one, the optical densities of the phenol or nitrobenzene solutions equilibrated with the adsorbent were divided by the optical density of the solution prepared with magnetic adsorbent stirring in water. Thus, the following equation was used:

$$\frac{A(\lambda)}{E_m(\lambda)l} = \frac{\varepsilon_a(\lambda)}{E_m(\lambda)} C_a + c_m$$

The slope of the dependence is the equilibrium concentration of the adsorbate, while the cut-off segment on the ordinate axis is the relative concentration of fine magnetite particles. The second way simplifies the parameters' uncertainty estimation due to known expressions for the linear regression. An example of optical density spectral dependencies processing from Figure 3 is presented in Figure 5.

It is worth emphasizing that the magnetite light absorption spectrum depends on the size distribution of its particles, which could vary from one experiment to another, leading to additional uncertainties in concentration. This notion makes the spectral dependence decomposition significantly inaccurate in the range of small concentrations of nitrobenzene or phenol.

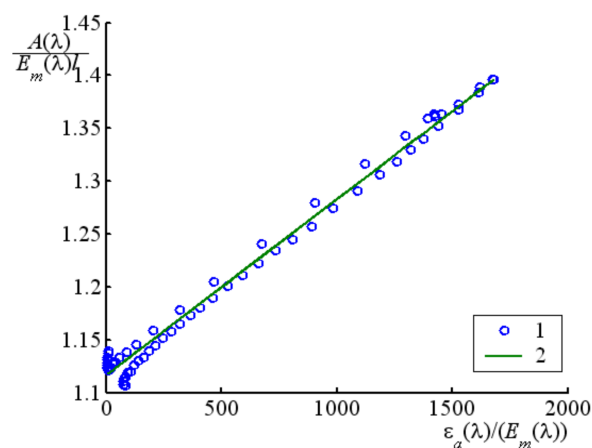


Figure 5. An example of the spectra shown in Figure 3, processing for the adsorbate concentration determination in the solution equilibrated with the magnetic adsorbent with stirring. Circles (1) show the calculated function from the spectrum, and the line (2) is a linear approximation.

3. Results and Discussion

3.1. Magnetic Adsorbents' Porous Structure

Low-temperature nitrogen adsorption isotherms are shown in Figure 6, and the results of the porous structure characterization are presented in Table 1. A type IV isotherm (IUPAC classification), characterized by a capillary condensation hysteresis loop due to a high mesopore fraction, is observed for every sample. Activated carbon AG-3 has a higher specific surface and specific pore volume than BAU-A. The macropore fraction in AG-3 is also higher. The parameters of AG-3 activated carbon's meso- and macroporous structure correlate with its better ability to adsorb methylene blue from concentrated solution. The BAU-A adsorbent performs better than AG-3 in benzene vapor adsorption due to higher specific micropore volume. The saturated benzene vapor adsorption and methylene blue adsorption capacities of BAU-A are comparable to those determined in [26] and [27], respectively. Deviations can be explained taking into account the differences in granulometric composition. The porous structure parameters of AG-3 are close to the ones determined in [28]. The hysteresis loops on the nitrogen adsorption isotherm is of the H4 type for both initial activated carbons, evidencing slit-shaped mesopore domination.

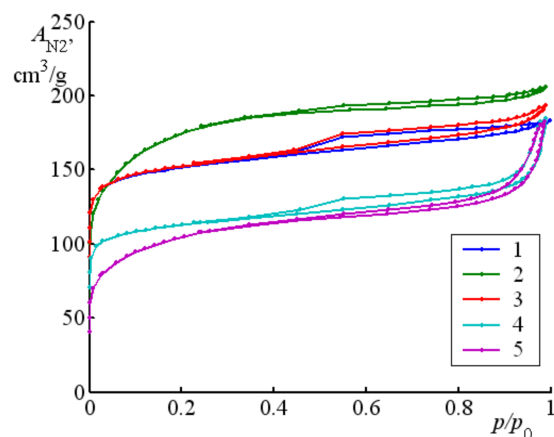


Figure 6. Low-temperature nitrogen isotherm adsorption. The samples' numeration matches Table 1.

Magnetite deposition does not lead to a specific surface area and a specific pore volume decrease in case of iron (II) sulfate and potassium oxalate solutions of volumes 10 and 15 mL, respectively. If the initial volumes were 20 and 30 mL, respectively, the specific surface and specific pore volume would decrease. The decrease in porosity characteristics

is accompanied by a decrease in the adsorption capacity for benzene-saturated vapors and methylene blue, adsorbed from the aqueous medium. At the same time, one observes a change of the hysteresis loop type to H3, which is usual for wedge-shaped mesopores. The changes observed could be interpreted as partial closing of the small pores with deposited magnetite. A significant part of the magnetite is deposited into macropores in the case of AG-3 activated carbon, which is seen in the reduction of their fraction in overall porosity. The magnetite growth inside the macropores and on the outer surface causes the evolution of wedge-shaped pores and the increase in average pore size.

3.2. Phenol and Nitrobenzene Adsorption

The isotherms of phenol and nitrobenzene adsorption from aqueous medium on BAU-A activated carbon are shown on Figures 7 and 8, respectively. The adsorption value for both adsorbates tends to the constant value in the limit of high concentrations, which is typical for Langmuir adsorption. The results in the Langmuir equation coordinates are shown in Figures 9 and 10, respectively, proving the assumption. The Langmuir parameters for nitrobenzene adsorption are $q_{\infty} = 2.04 \pm 0.02$ mmole/g and $K = (20 \pm 10)$ L/mmole. In the case of phenol adsorption, the parameters are $q_{\infty} = 1.46 \pm 0.06$ mmole/g and $K = 7 \pm 4$ L/mmole. The nitrobenzene adsorption constant is higher than the phenol one, correlating with its higher hydrophobicity and lower solubility in water. The nitrobenzene and phenol adsorption limiting values are close.

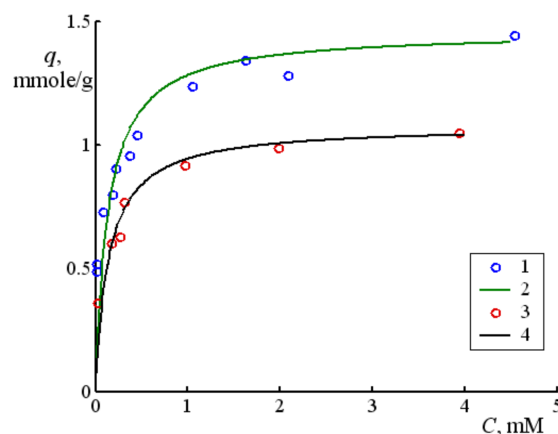


Figure 7. Experimental isotherms of phenol adsorption on BAU-A activated carbon (1) and magnetic adsorbent on its base (3) and their approximation with Langmuir equation (2,4).

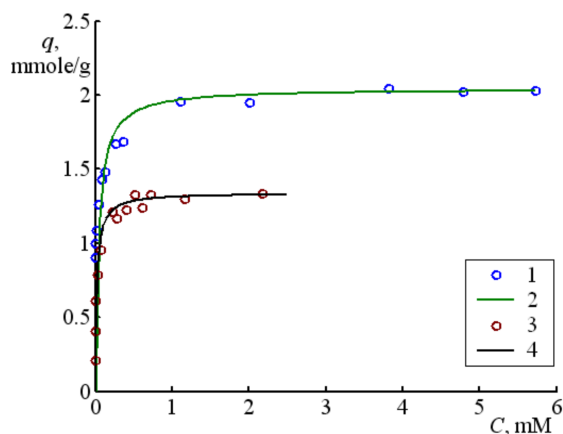


Figure 8. Nitrobenzene adsorption experimental isotherms on BAU-A activated carbon (1) and magnetic adsorbent on its base (3) and their approximation with Langmuir equation (2,4).

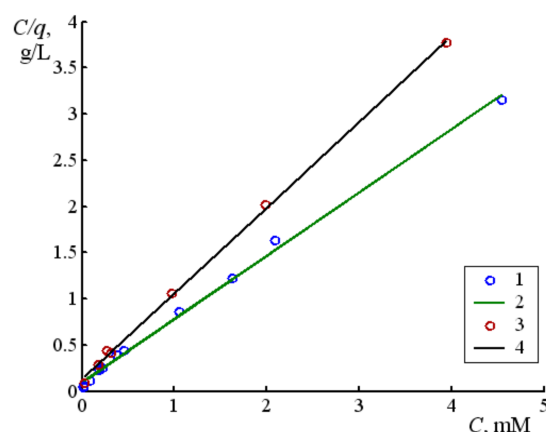


Figure 9. Phenol adsorption experimental isotherms on BAU-A activated carbon (1) and magnetic adsorbent on its base (3) in the Langmuir equation coordinates and their linear approximations (2,4).

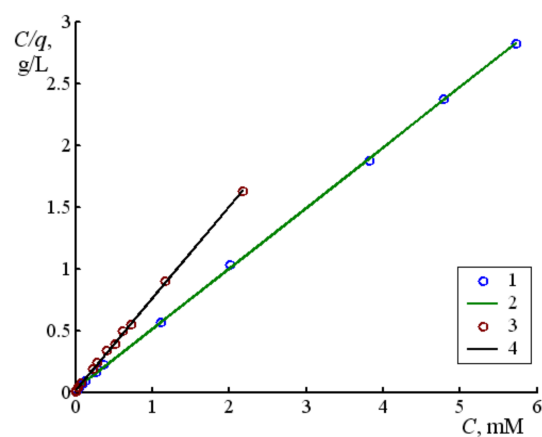


Figure 10. Nitrobenzene adsorption experimental isotherms on BAU-A activated carbon (1) and magnetic adsorbent on its base (3) in the Langmuir equation coordinates and their linear approximations (2,4).

Adsorption isotherms of phenol and nitrobenzene on the magnetic adsorbent prepared from BAU-A are presented in Figures 7 and 8, while linearized dependencies are shown in Figures 9 and 10. One is able to conclude that a Langmuir character remains after magnetite deposition. Langmuir adsorption parameters are $q_{\infty}=1.34 \pm 0.02$ mmole/g and $K = 47 \pm 30$ L/mmole for nitrobenzene and $q_{\infty}=1.08 \pm 0.04$ mmole/g and $K = 7 \pm 3$ L/mmole for phenol. The observed uncertainty of the adsorption constants could be linked to non-ideal uniformity of the adsorbents' surface that is one of the key assumptions of the Langmuir adsorption model. Comparison of adsorption limits between the magnetic adsorbent and initial activated BAU-A carbon makes their diminishing by 27% for phenol and 34% for nitrobenzene evident. The decrease observed is close to the relative decrease in specific surface area caused by magnetite deposition. Comparing the overall adsorption performance of the initial and modified adsorbent, one concludes that magnetite deposition does not lead to a significant worsening of this property.

4. Conclusions

The present work describes magnetic adsorbent synthesis with the previously suggested method of iron (II) oxalate deposited on a carbonaceous matrix via thermolysis and presents the results of research on their porous structure and adsorption properties. The method applied provides a high yield of the magnetic product. We showed that magnetite deposition does not deteriorate the activated carbon adsorption performance, with specific surface and phenol adsorption limit decreasing by 26% and nitrobenzene adsorption limit

decreasing by 34%. We are planning to optimize the synthetic approach in future research in order to improve the adsorption and mechanical performance of the product.

Author Contributions: Conceptualization, A.Z. and A.K. (Alexander Kalenskii); methodology, A.I. and A.K. (Alexander Krechetov); investigation, D.S. and A.Z.; writing—original draft preparation, A.Z.; writing—review and editing, A.K. (Alexander Kalenskii); supervision, A.K. (Alexander Kalenskii). All authors have read and agreed to the published version of the manuscript.

Funding: This research received no external funding.

Institutional Review Board Statement: Ethical review and approval are not applicable for this study.

Informed Consent Statement: Not applicable.

Data Availability Statement: The data presented in this study are available on request from the corresponding author.

Acknowledgments: The authors are grateful to Elena Pomesyachnaya for her help in the samples' preparation and Yulia Dudnikova for low-temperature nitrogen adsorption analysis.

Conflicts of Interest: The authors declare no conflict of interest.

References

1. Liu, M.; Ye, Y.; Ye, J.; Gao, T.; Wang, D.; Chen, G.; Song, Z. Recent Advances of Magnetite (Fe₃O₄)-Based Magnetic Materials in Catalytic Applications. *Magnetochemistry* **2023**, *9*, 110. [[CrossRef](#)]
2. Kaur, A.; Kaur, M.; Singh, V.; Vyas, P. Nanocomposites of Ferrites with TiO₂, SiO₂ and Carbon Quantum Dots as Photocatalysts for Degradation of Organic Pollutants and Microbes. *Magnetochemistry* **2023**, *9*, 127. [[CrossRef](#)]
3. Gao, X.; Zhang, Y.; Dai, Y.; Fu, F. High-performance magnetic carbon materials in dye removal from aqueous solutions. *J. Solid State Chem.* **2016**, *239*, 265–273. [[CrossRef](#)]
4. Panga, S.C.; Khoh, W.H.; Chin, S.F. Synthesis and Characterization of Magnetite/Carbon Nanocomposite Thin Films for Electrochemical Applications. *J. Mater. Sci. Technol.* **2011**, *27*, 873–878. [[CrossRef](#)]
5. Kharlyamov, D.A.; Fazullin, D.D.; Mavrin, G.V. Method of obtaining magnetic composite sorbent for wastewater treatment from ions of heavy metals and petroleum products. Patent RU 2626363, 26 July 2017. (In Russian).
6. Azizov, A.A.; Sulaiman, M.A.; Akhmadov, V.M.; Alosmanov, R.M.; Bunyad-Zadeh, I.A.; Magerramov, A.M. Porous Magnetic Sorbent. U.S. Patent 9011695, 21 April 2015.
7. Moscatelli, D.; Masi, M.; Pesce, R.M. Amphiphilic Magnetic Nanoparticles and Aggregates to Remove Hydrocarbons and Metal Ions and Synthesis Thereof. Patents WO 2015/177710, 18 May 2015.
8. Kydraliev, K.A.; Jurishcheva, A.A.; Pomogajlo, A.D.; Dzhardimalieva, G.I.; Pomogajlo, S.I.; Golubeva, N.D. Magnetic Composite Adsorbent. Patent RU 2547496, 10 April 2015.
9. Tamjidi, S.; Esmaeili, H.; Moghadas, B.K. Application of magnetic adsorbents for removal of heavy metals from wastewater: A review study. *Mater. Res. Express* **2019**, *6*, 102004. [[CrossRef](#)]
10. Kazemi, E.; Dadfarnia, S.; Shabani, A.M.H.; Hashemim, P.S. Synthesis of 2-mercaptobenzothiazole/magnetic nanoparticles modified multi-walled carbon nanotubes for simultaneous solid-phase microextraction of cadmium and lead. *Int. J. Environ. Anal. Chem.* **2017**, *97*, 743–755. [[CrossRef](#)]
11. Sedghi, R.; Heidari, B.; Kazemi, S. Novel magnetic ion-imprinted polymer: An efficient polymeric nanocomposite for selective separation and determination of Pb ions in aqueous media. *Environ. Sci. Pollut. Res.* **2018**, *25*, 26297–26306. [[CrossRef](#)]
12. Zhang, C.; Sui, J.; Li, J.; Tang, Y.; Cai, W. Efficient removal of heavy metal ions by thiol-functionalized superparamagnetic carbon nanotubes. *Chem. Eng. J.* **2012**, *210*, 45–52. [[CrossRef](#)]
13. Chen, D.; Chen, C.; Shen, W.; Quan, H.; Chen, S.; Xie, S.; Luo, X.; Guo, L. MOF-derived magnetic porous carbon-based sorbent: Synthesis, characterization, and adsorption behavior of organic micropollutants. *Adv. Powder Technol.* **2017**, *28*, 1769–1779. [[CrossRef](#)]
14. Manoochehri, M.; Naghibzadeh, L.A. Nanocomposite Based on Dipyritydylamine Functionalized Magnetic Multiwalled Carbon Nanotubes for Separation and Preconcentration of Toxic Elements in Black Tea Leaves and Drinking Water. *Food Anal. Methods* **2017**, *10*, 1777–1786. [[CrossRef](#)]
15. Huang, Y.; Peng, J.; Huang, X. One-pot preparation of magnetic carbon adsorbent derived from pomelo peel for magnetic solid-phase extraction of pollutants in environmental waters. *J. Chromatogr. A* **2018**, *1546*, 28–35. [[CrossRef](#)]
16. Zhao, W.; Tian, Y.; Chu, X.; Cui, L.; Zhang, H.; Li, M.; Zhao, P. Preparation and characteristics of a magnetic carbon nanotube adsorbent: Its efficient adsorption and recoverable performances. *Sep. Purif.* **2021**, *257*, 117917. [[CrossRef](#)]
17. Kefeni, K.K.; Mamba, B.B.; Msagati, T.A.M. Application of spinel ferrite nanoparticles in water and wastewater treatment: A review. *Sep. Purif.* **2017**, *188*, 399–422. [[CrossRef](#)]
18. Le, V.T.; Tran Thi, K.N.; Tran, D.L.; Le, H.S.; Doan, V.D.; Bui, Q.D.; Nguyen, H.T. One-pot synthesis of a novel magnetic activated carbon/clay composite for removal of heavy metals from aqueous solution. *J. Dispers. Sci. Technol.* **2019**, *40*, 1761–1776. [[CrossRef](#)]

19. Kurmangazhi, G.; Tazhibayeva, S.M.; Musabekova, K.B.; Levin, I.S.; Kuzin, M.S.; Ermakova, L.E.; Yu, V.K. Preparation of Dispersed Magnetite–Bentonite Composites and Kazcaine Adsorption on Them. *Colloid J.* **2021**, *83*, 343–351. [[CrossRef](#)]
20. Zubrik, A.; Matik, M.; Lovás, M.; Danková, Z.; Kaňuchová, M.; Hredzák, S.; Briančin, J.; Šepelák, V. Mechanochemically Synthesised Coal-Based Magnetic Carbon Composites for Removing As(V) and Cd(II) from Aqueous Solutions. *Nanomaterials* **2019**, *9*, 100. [[CrossRef](#)]
21. Reynel-Ávila, H.E.; Camacho-Aguilar, K.I.; Bonilla-Petriciolet, A.; Mendoza-Castillo, D.I.; González-Ponce, H.A.; Trejo-Valencia, R. Engineered Magnetic Carbon-Based Adsorbents for the Removal of Water Priority Pollutants: An Overview. *Adsorp. Sci. Technol.* **2021**, *2021*, 9917444. [[CrossRef](#)]
22. Hermanek, M.; Zboril, R.; Mashlan, M.; Machala, L.; Schneeweiss, O. Thermal behaviour of iron(II) oxalate dihydrate in the atmosphere of its conversion gases. *J. Mater. Chem.* **2006**, *16*, 1273–1280. [[CrossRef](#)]
23. Kalenskii, A.V.; Zvekov, A.A.; Popova, A.N.; Anan'ev, V.A.; Grishaeva, O.V. Production of Magnetic Carbon Materials during Decomposition of Iron Salts Deposited on a Porous Carbon Matrix. *Russ. J. Appl. Chem.* **2021**, *94*, 486–490. [[CrossRef](#)]
24. Morris, R.V.; Lauer, H.V., Jr.; Lawson, C.A.; Gibson, E.K., Jr.; Nace, G.A.; Stewart, C. Spectral and Other Physicochemical Properties of Submicron Powders of Hematite (α -Fe₂O₃), Maghemite (γ -Fe₂O₃), Magnetite (Fe₃O), Goethite (α -FeOOH), and Lepidocrocite (γ -FeOOH). *J. Geophys. Res.* **1985**, *90*, 3126–3144. [[CrossRef](#)]
25. Bershtein, I.Y.; Kaminskii, Y.L. *Spectrophotometric Analysis in Organic Chemistry*; Khimiya: Leningrad, Russia, 1975; pp. 26–45. (In Russian)
26. Fazylova, G.F.; Valinurova, E.R.; Khatmullina, R.M.; Kudasheva, F.K. Fenol derivatives sorption parameters on various carbon materials. *Sorbtsionnye I Khromatograficheskie Protsessy* **2013**, *13*, 728–735. (In Russian)
27. Khokhlova, T.D.; Khien, L.T. Dyes' adsorption on activated carbons and graphitized soot. *Vestn. Moskov. Univ. Ser. 2 Khimiya* **2007**, *48*, 157–161. (In Russian)
28. Krasnova, T.A.; Belyaeva, O.V.; Kirsanov, M.P. Use of activated carbons in water preparation and water removal processes. *Food Process. Tech. Technol.* **2012**, *3*, 46–56.

Disclaimer/Publisher's Note: The statements, opinions and data contained in all publications are solely those of the individual author(s) and contributor(s) and not of MDPI and/or the editor(s). MDPI and/or the editor(s) disclaim responsibility for any injury to people or property resulting from any ideas, methods, instructions or products referred to in the content.